

A NUMERICAL SIMULATION OF METAL INJECTION MOULDING

NUMERIČNE SIMULACIJE BRIZGANJA KOVINSKIH PRAŠNATIH MATERIALOV

Boštjan Berginc¹, Miran Brezočnik², Zlatko Kampuš¹, Borivoj Šuštaršič³

¹University of Ljubljana, Faculty of Mechanical Engineering, 1000 Ljubljana, Aškerčeva 6, Slovenia

²University of Maribor, Faculty of Mechanical Engineering, 2000 Maribor, Smetanova ulica 17, Slovenia

³Institute of Metals and Technology, 1000 Ljubljana, Lepi pot 11, Slovenia

Prejem rokopisa – received: 2008-03-18; sprejem za objavo – accepted for publication: 2008-10-10

Metal injection moulding (MIM) is already a well-established and promising technology for the mass production of small, complex, near-net-shape products. The dimensions and mechanical properties of MIM products are influenced by the feedstock characteristics, the process parameters of the injection moulding, as well as the debinding and the sintering. Numerical simulations are a very important feature of the beginning of any product or technology development. In the article two different techniques for measuring the rheological properties of MIM feedstocks are presented and compared. It was established that capillary rheometers are more appropriate for MIM feedstocks, while on the other hand, parallel-plate rheometers are only suitable for shear rates lower than 10 s^{-1} . Later on we used genetic algorithms to determine the model coefficients for some numerical simulation software. The results of the simulation of the filling phase and a comparison with the experimental results are presented in the article.

Keywords: metal injection moulding, numerical simulation, genetic algorithms

Brizganje kovinskih prašnatih materialov (MIM) je uveljavljena tehnologija, primerna za izdelavo majhnih, kompleksnih izdelkov visoke natančnosti. Dimenzije in mehanske lastnosti MIM-izdelkov so odvisne od lastnosti mešanic, procesnih parametrov brizganja, odstranjevanja veziva in sintranja.

Numerične simulacije so pri razvoju novih izdelkov oziroma tehnologij zelo pomembne. V prispevku je narejena primerjava in predstavitev dveh metod za merjenje reoloških lastnosti MIM mešanic. Ugotovljeno je bilo, da je kapilarni reometer primernejši za meritve pri višjih strižnih hitrostih, medtem ko je reometer z vzporedno ploščo primeren le za strižne hitrosti do 10 s^{-1} . V nadaljevanju je bila uporabljena metoda genetskih algoritmov za določitev koeficientov matematičnega modela, ki se uporablja v programski opremi za numerične simulacije brizganja. Na koncu so predstavljeni rezultati simulacije polnjenja orodne votline, narejena pa je tudi primerjava z eksperimentalnimi rezultati.

Ključne besede: brizganje kovinskih prašnatih materialov, numerične simulacije, genetski algoritmi

1 INTRODUCTION

Powder injection moulding (PIM) or metal injection moulding (MIM) is a combination of four sequential technological processes – mixing, injection moulding, debinding and sintering – all of which have an effect on the characteristics of the final parts. The feedstock, which has to be as homogeneous as possible, is made by intensive mixing of the metal powder and the binder, and in the next phase a green part is made by injection moulding. Then the binder is removed from the green part in various debinding processes. The brown part that is produced retains its shape due to the friction between the particles of the metal powder. This part is very brittle and needs to be sintered carefully to achieve its final sintered density and the desired mechanical, chemical and dimensional properties. The final properties of the product can be further improved with additional heat and mechanical treatments.^{1,2}

A rheological characterisation of the selected feedstock, ADVAMET 316L, was performed using a parallel-plate and a capillary rheometer. On the basis of the viscosity measurement the coefficients of the

selected mathematical model were then determined and used for a numerical simulation with the Moldflow simulation software.

2 MIM FEEDSTOCK CHARACTERISATION

2.1 Viscosity measurement

MIM feedstocks usually consist of a binder, which is based on polymers and waxes, and metal particles. During the injection moulding their behaviour is similar to other shear thinning fluids. The increase in the shear rate causes the fluid's viscosity to decrease, which is well made use of in the injection-moulding process. A precise feedstock characterisation is thus needed for a complete understanding of the whole process as well as for finite-element-method-based (FEM-based) numerical simulations of injection moulding.

The viscosity of the ADVAMET 316L feedstock was measured with a Rheologic 5000 Twin Bore capillary rheometer and an Anton Paar Physica MCR 301 parallel-plate rheometer. The material ADVAMET 316L consists of a wax-polymer binder and spherical, austenitic stainless-steel powder particles with a diameter

smaller than 18 μm. L stands for the low carbon content, which is less than 0.03 %.

The Anton Paar rheometer was used to measure the melts' viscosity using a cylindrical rotating plate of diameter 21 mm. The shear stress is measured from the torque, which appears because of the material's resistance to flow. The sample of material was placed between the rotating disk and the immovable plate at a distance of 0.98 mm, while the temperature was held at 195 °C. The accuracy of this method is based on the supposition that the velocity of the melt at the rotating disk is the same as the velocity of the disk. The errors during the measurement are unavoidable at high velocities and for low-viscosity materials. The disadvantage of this method is that the shear rate is not the same throughout the whole cross-section of the disk. Therefore, the cone plate disks are more appropriate, but here a minimum distance between the rotating cone and the immovable plate that is only a few micrometers must be achieved. The metal particles in the MIM feedstock could hinder the disk rotation, and so a torque measurement would be incorrect. The basic principles of a viscosity measurement acquired with a parallel-plate rheometer are presented in **Figure 1**.

The apparent shear rate is calculated from the angle velocity ω , the distance δ and the plate radius r using the following relation:

$$\dot{\gamma}_{ap} = \frac{r \cdot \omega}{\delta} \quad (1)$$

while the shear stress τ is calculated from the torque M , measured on the axis using equation (2).

$$\tau = \frac{3M}{2\pi r} \quad (2)$$

These rheometers can be used for determining viscoelastic information about the tested material (creep test, zero-shear viscosity, relaxation modulus G , elastic modulus G' and viscous modulus G''), the data about the molecular structure and the rheological characteristics during a prolonged exposure to shear stress.^{3,4} **Figure 2** shows the shear-rate intervals for viscosity measurements with different measuring methods.

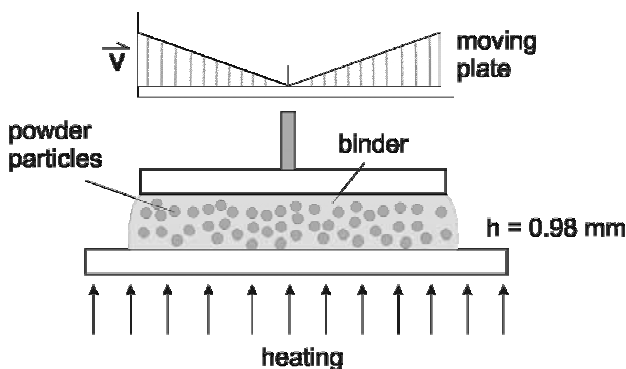


Figure 1: Parallel-plate rheometer
Slika 1: Reometer z vzporedno ploščo

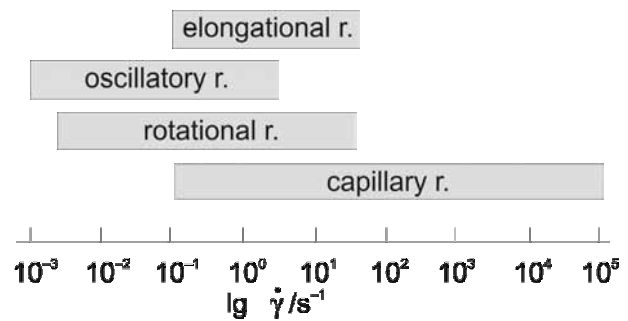


Figure 2: Shear rate for viscosity measurements with different methods

Slika 2: Območja strižnih hitrosti pri različnih metodah merjenja viskoznosti

With the capillary rheometer the volume flow rate of the extruded melt through a capillary of diameter 1 mm and length 20 mm was measured according to ISO 114433. The measurements were made in the temperature interval between 180 °C and 200 °C, while the shear rate was between 10⁻¹ and 10 000 s⁻¹. This method is appropriate for viscosity measurements on polymer materials, because the real conditions during the injection moulding and extrusion are similar to those during the viscosity measurement. The viscosity can be measured at high shear rates, and at the same time the measurements are accurate enough for further evaluation. The biggest disadvantages are a pressure drop at the entrance to the capillary, melt heating, and the dependence of viscosity on pressure. For an exact determination of the viscosity for non-Newtonian fluids the Weissenberg-Rabinowitsch and Bagly corrections are used (ISO 11443). The Bagley correction is used to determine the true shear stress due to the pressure drop at the entrance and exit of the capillary die.

The viscosity of non-Newtonian fluids calculated from the flow rate Q and shear stress τ , which is determined from the pressure drop Δp in the capillary, is the so-called apparent viscosity η_{ap} . The shear rate $\dot{\gamma}_{ap}$ and shear stress τ are calculated using equations (3) and (4):

$$\dot{\gamma}_{ap} = \frac{32Q}{\pi \cdot D^3} \quad (3)$$

$$\tau = \frac{\Delta p \cdot D}{4 \cdot L} \quad (4)$$

and so the apparent viscosity is

$$\eta_{ap} = \frac{\tau}{\dot{\gamma}_{ap}} \quad (5)$$

where D and L are the capillary diameter and the length. The Newtonian fluids are independent of shear rate, while the viscosity of the viscoelastic fluids is lowered by the increased shear rate. Thus, the Rabinowitsch correction for capillary-die rheometers is used afterwards to determine the true viscosity, which is calculated using equation (6):

$$\dot{\gamma} = \frac{\dot{\gamma}_{ap}}{4} \left(3 + \frac{d \lg \dot{\gamma}_{ap}}{d \lg \tau} \right) \quad (6)$$

where $d \lg \dot{\gamma}_{ap} / d \lg \tau$ is the slope of the curve $\lg \dot{\gamma}_{ap} = f(\lg \tau)$. The difference between the apparent viscosity and the true viscosity is usually smaller than 30 %. The apparent viscosity is accurate enough for determining the fluid's behaviour, and usually the true viscosity does not need to be calculated. On the other hand, it is recommended that we determine the true viscosity for an analysis with numerical simulations; however, in our case we did not have the resources to perform three viscosity measurements using different D/L capillary ratios in order to use the Bagley correction. Instead, we used the apparent viscosity for a numerical simulation of the filling phase using a Moldflow Plastic Insight 5.0. The comparison between the apparent viscosity and the true viscosity is presented in **Figure 3**.

Figures 4 and 5 show the results of viscosity measurements for the selected feedstock using both methods. The viscosity measurement using a parallel plate (**Figure 4**) shows that the shear stress increases only to the point when the shear rate reaches 10 s^{-1} , after which it decreases. The shear rates during high-pressure MIM can be up to 1000 times the stated shear rate. As regards the measurements, we would like to approach the actual processing conditions, but this was not possible with this method. The decrease of the shear stress could be the result of a thin layer of the binder near the wall (wall slip), which acts as a lubricant and lowers the friction of the fluid flow or because of a fracture of the test sample's edge. These effects probably already appeared when the shear rate was 5 s^{-1} , because above this value the shear stress increases more slowly.

A serious edge effect can appear with high-viscosity fluids like polymers and MIM feedstocks, where at low shear rates $\dot{\gamma} < 10 \text{ s}^{-1}$ the sample appears to cut at the midplane. Before this effect is visible it can be detected by a drop in the torque ⁵. The wall-slip effect can be partially avoided by using a roughened parallel-plate

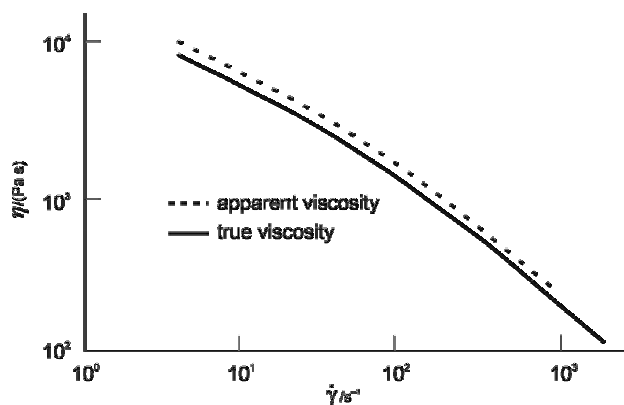


Figure 3: An example of the apparent and the true viscosity calculated using the Rabinowitsch correction

Slika 3: Primer navidezne in prave strižne viskoznosti, izračunane z Rabinowitschevo korekcijo

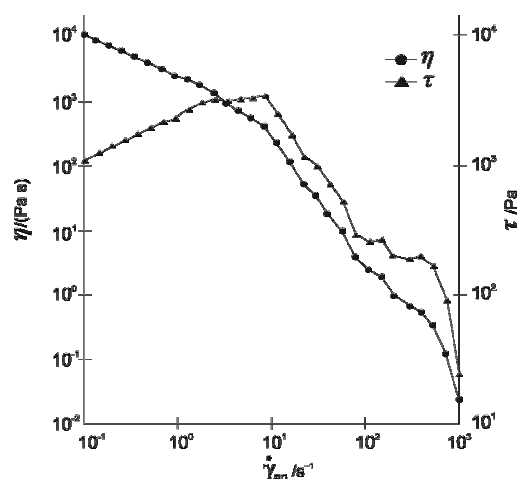


Figure 4: Viscosity and shear stress of ADVAMET 316L feedstock measured with the parallel-plate rheometer.

Slika 4: Z reometrom z vzporedno ploščo izmerjena strižna viskoznost in napetost za material ADVAMET 316L

surface or by making grooves and notches ⁶. The wall-slip effect of filled materials was investigated in several studies ⁶⁻⁹. For shear rates higher than 10 s^{-1} , when a critical shear stress is probably reached, the melt fractures and the shear stress and viscosity decrease rapidly. The adhesion and cohesion between the molecules is lower for materials filled with solid particles. Therefore, the shear stress decreases or oscillates when the adhesion restores or breaks ³.

The viscosity determined with the capillary rheometer decreases linearly in a log-log diagram in the interval between 10 s^{-1} and 10000 s^{-1} (**Figure 5**). After the comparison of the two methods for the viscosity determination of MIM feedstocks we established that the parallel-plate method is only suitable for lower shear

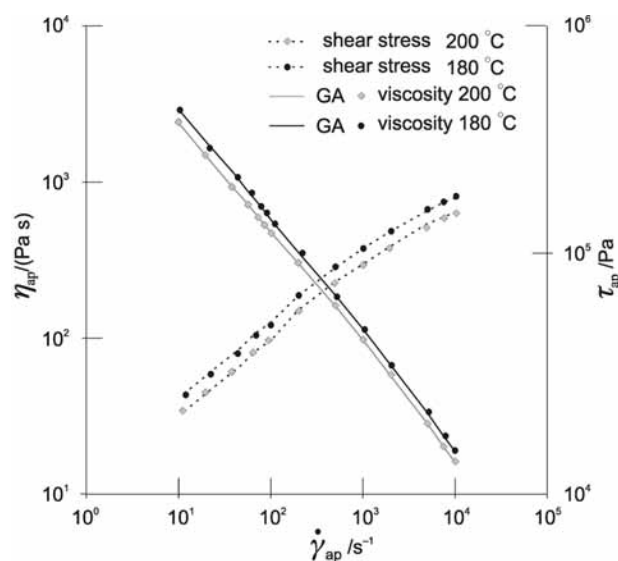


Figure 5: Viscosity and shear stress of ADVAMET 316L feedstock measured with the capillary rheometer

Slika 5: S kapilarnim reometrom izmerjena strižna viskoznost in napetost za material ADVAMET 316L

rates, while higher share-rate measurements should be made with capillary rheometers. The conditions in the latter method are similar to the real process conditions.

2.2 The determination of the model coefficients for a numerical simulation

To successfully perform a numerical simulation the rheological and thermal data as well as a pressure-volume-temperature (pVT) diagram must be obtained. In this investigation we focused on a characterisation of the feedstock's rheological properties; the determination of the pVT diagram for this material is set for a future investigation.

According to a recent paper ¹⁰ it is possible to use commonly available commercial software for the simulation of thermoplastic injection moulding to make useful numerical simulations of the MIM process because the material properties of the thermoplastic and metal feedstocks are quite similar, from the point of view of numerical simulations.

For numerical simulations of the injection-moulding process it is normal to use two mathematical models, which show the dependence of the shear viscosity, η , the shear rate, $d\gamma/dt$, and the temperature, T . The first one is the so-called Cross-WLF model, and the other one is a second-order model. From these two mathematical models we chose the latter, because it is more suitable for materials with a decreased viscosity across the whole range of shear rates (**Figure 5**). The second-order model is given with the following equation:

$$\ln \eta = A + B \cdot \ln \dot{\gamma} + C \cdot T + D (\ln \dot{\gamma})^2 + E \cdot T \cdot \ln \eta + F \cdot T^2 \quad (7)$$

where η , $d\gamma/dt$ and T are the viscosity (Pa s), shear rate (s^{-1}) and temperature ($^{\circ}C$), respectively, while A to F are data-fitted coefficients.

The coefficients were determined using genetic algorithms (GAs) (Table 1). The coding of the organisms was as follows: the initial random population $P(t)$ consisted of real-valued vectors (organisms) and of the constants A , B , C , D , and F . The variable t is the generation time. The absolute deviation $D(i, t)$ of an individual organism i in generation time t was introduced as the fitness measure. It was defined as:

$$D(i, t) = \sum_{j=1}^n |E(j) - P(i, j)| \quad (8)$$

where $E(j)$ is the experimental value for the measurement j , $P(i, j)$ is the predicted value returned by the individual organism i for the measurement j , and n is the maximum number of measurements. Of course, the predicted value $P(i, j)$ is calculated by inserting the constants A to F into the second-order model (7). Eq. (8) is a standard fitness measure for solving regression problems, proposed by Koza ¹¹. The aim of the optimisation task is to find such a model (7) that Eq. (9) would give as low an absolute deviation as possible. However, because it is not necessary that the smallest values of

the above equation also mean the smallest percentage deviation of this model, the average absolute percentage deviation of all the measurements for an individual organism i was defined as:

$$\Delta(i) = \frac{D(i, t)}{|E(j)|n} \cdot 100 \% \quad (9)$$

The altering of the population $P(t)$ is affected by reproduction, crossover, and mutation. For the crossover operation, two parental vectors are selected randomly. Then the crossover takes place between two randomly selected parental genes having the same index. Two offspring genes are created according to an extended intermediate crossover, considered by Mühlenbeim and Schlierkamp-Voosen ¹². In the mutation operation, one parental vector is selected randomly. Then, the mutation takes place in one randomly selected parental gene. In both crossover and mutation the number of crossover and mutation operations performed on parental vector(s) is selected randomly.

The evolutionary parameters were as follows: population size, 100; maximum number of generations to be run, 4000; probability of reproduction, 0.1; probability of crossover, 0.3; and probability of mutation, 0.6. The method of selection for all three genetic operations was a tournament selection with a group size of 4.

Table 1: Coefficients of the second-order model determined with a GA

Preglednica 1: Koeficienti modela drugega reda, določeni z GA

A	16.0317	C	$-5.52 \cdot 10^{-2}$	E	$1.01 \cdot 10^{-3}$
B	$-7.81 \cdot 10^{-1}$	D	$-1.16 \cdot 10^{-2}$	F	$1.03 \cdot 10^{-4}$

3 EXPERIMENTS

The experiments were made on a KraussMaffei KM50/220c injection-moulding machine (**Figure 6**),



Figure 6: A photograph of the testing area with the injection-moulding machine and the surveyor's chain

Slika 6: Slika preizkuševališča s strojem za brizganje in merilno verigo



Figure 7: Green and sintered specimens used for the analyses
Slika 7: Zeleni in sintrani kos, uporabljen za analizo

with a standard 30-mm diameter screw. The pressure and temperature in the cavity were measured using Kistler's sensor 6190A0,8 with a NiCr-Ni Type-K thermoelement, positioned 20 mm from the gate. The pressure charge signal was then amplified with Kistler's charge amplifier 5039A222, which was connected to the PC through a digital acquisition card PCI-9114(A) DG/HG. We were able to measure the pressure in the cavity with the pressure sensor and then compare it to the machine's injection pressure. The pressure data was later used for a comparison with the numerical simulation.

The test specimen used for the injection-moulding analysis is presented in **Figure 7**. The coefficients of the second-order model were used for the creation of new material in the Moldflow database. Other feedstock characteristics that are necessary for a numerical simulation are the thermal conductivity $\lambda = 1 \text{ W/mK}$ and the specific heat $c_p = 950 \text{ J/(kg K)}$. The recommended processing parameters for this feedstock are presented in **Table 2**. The dimensions of the part are $(55 \times 9 \times 5) \text{ mm}$ and the hole diameter is 5 mm.

Table 2: Recommended processing parameters for ADVAMET 316L
Preglednica 2: Priporočene vrednosti procesnih parametrov za ADVAMET 316L

Parameter	value
Material temperature	190 °C
Mold temperature	45–50 °C
Injection speed	< 8 cm ³ /s
Ejection temperature	60 °C

For the meshing we used Moldflow's 3D meshing with tetrahedral elements, with a total number of around 24,000. The solver used for the analysis was Navier-Stokes with simulation of the inertia effect. Because the $p\nu T$ data was not determined, only the

filling phase of the injection-moulding process was preformed.

4 RESULTS

In **Figure 8** it can be seen that the injection time can be quite long, although the material is filled with metal powder. We successfully filled the cavity with an injection speed as low as 1 cm³/s, with an injection time of around 3 s. However, the parts that were filled for more than 1.5 s had explicit weld lines and so longer injection times are not recommended. From our studies we concluded that the lowest injection speed for thick parts should be around 4 cm³ /s, and for thinner parts around 8 cm³/s.

Several testing conditions were examined during the result comparison. From **Figure 9** it can be seen that the material flows easily, as the injection pressure necessary to fill the whole part is low (170 bar). A very low pressure is needed to fill the part up to the hole (80 bar). To overcome the resistance due to a thinner flow path, a higher pressure must be applied. Simulations show that when the injection time is 2 s, the necessary injection pressure to fill the whole part is 160 bar, while the pressure inside the cavity, where the sensor is, is 85 bar (**Figure 9**). The experiments showed that the necessary injection pressure at the defined injection time is 120 bar, while the cavity pressure rises to around 80 bar. Longer injection times demand higher pressures to fill the cavity. We can see that the cavity pressure during the simulation and in the experiment is almost the same. The larger difference among the hydraulic pressures is probably a result of its dependence on the type and size of the machine. Nevertheless, the results of the numerical simulations are in good agreement with the experiments.

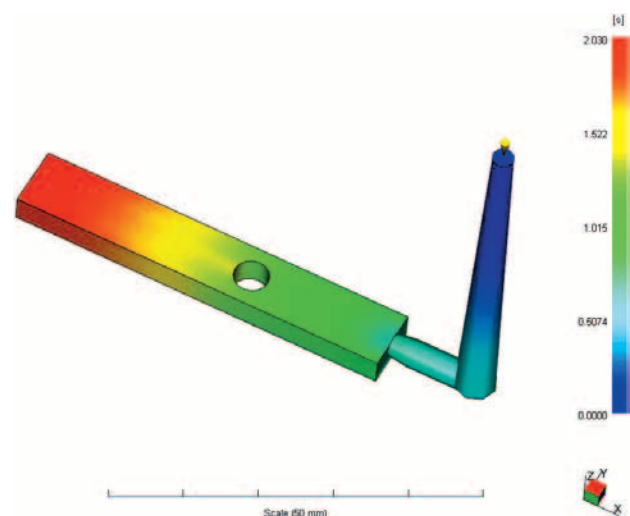


Figure 8: Simulation of the injection time of ADVAMET 316L
Slika 8: Z numerično simulacijo izračunan čas brizganja za ADVAMET316L

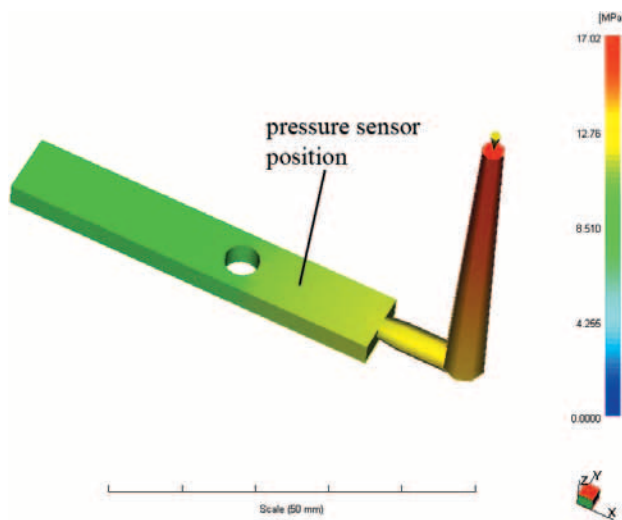


Figure 9: Simulation of injection pressure at the end of filling
Slika 9: Z numerično simulacijo izračunan tlak brizganja ob zapolnitvi orodne votline

During the experiment the temperature inside the cavity was also measured. Because of the material's high thermal conductivity the cooling times are rather low, even though the part is 5 mm thick. The part cooled almost to the mould temperature (48 °C) in around 30 s. The simulated cooling time and cooling time of the experiments were well correlated, because the results were practically identical. In **Figure 10** we can see that after 15 s the temperature inside the part is still 80 °C, while the mould temperature is 45 °C.

This practical experiment taught us that the part retains its shape and tolerances better if it is cooled almost to the mould temperature. If the part were to be ejected when the temperature of the core was higher than 80 °C, the part's shape retention would be reduced and this would result in bending and distortion. The optimal cooling time for this part would be between 20 s and 25 s.

5 CONCLUSIONS

In our investigations we established that Moldflow software can be used for numerical simulations of MIM materials. We successfully applied a GA to determine the coefficients of the numerical viscosity model and the simulated filling process of the injection phase using the apparent viscosity. For a confirmation of the numerical simulations the experiments of the injection-moulding process were performed.

The viscosity was measured using parallel-plate and capillary rheometers, and the latter proved to be the only one suitable for viscosity measurements of high viscosity MIM feedstocks. The next steps in our research will be

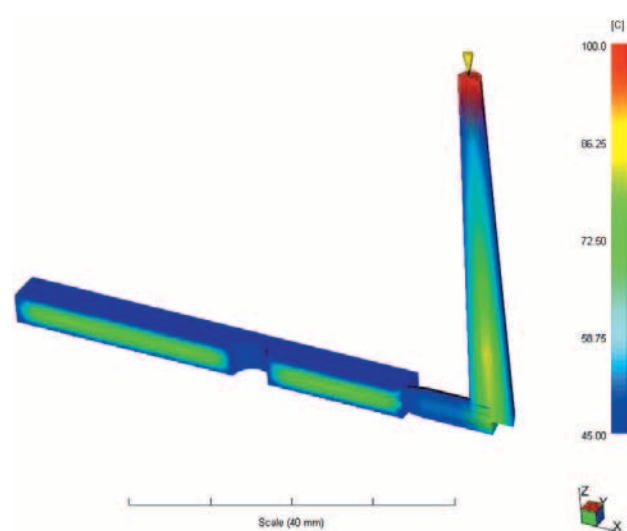


Figure 10: 3D temperature of MIM part, cooling time 15 s
Slika 10: Temperaturni profil MIM izdelka, pri času ohlajanja 15 s

measuring the $p-v-T$ data, a determination of the true shear rate, the use of GAs for other mathematical models and comparing the numerically simulated results with experiments.

Acknowledgements

The authors wish to thank CEAST S.p.A., Italy and the Jožef Stefan Institute, Ljubljana, for the viscosity measurements and Tecos, the Slovenian tool and development centre, Celje, for lending us the Moldflow license.

6 REFERENCES

- ¹ R. M. German: Powder Injection Moulding, New Jersey, MPIF, 1990
- ² R. M. German, A. Bose: Injection Molding of Metals and Ceramics, New Jersey, MPIF, 1997
- ³ R. W. Whorlow: Rheological Techniques 2nd edition, Ellis Horwood, 1992
- ⁴ M. Rides: Rheological characterisation of filled materials: a review, NPL Report DPEC-MPR 013, Teddington, UK, 2005
- ⁵ C. W. Macosko: Rheology, principles, measurements and applications, New York, Wiley-VCH inc., 1994.
- ⁶ H. A. Barnes: *J. Non-Newtonian Fluid Mech.*, 56 (1995), 221–251
- ⁷ T. H. Kwon, S. Y. Ahn: *Powder Technol.*, 85 (1995), 45–55
- ⁸ U. Yilmazer, D. M Kalyon: ANTEC, 1989, 1682–1686
- ⁹ D. M. Kalyon: *J. Mater. Process. Manuf. Sci.*, 2 (1993), 159–187
- ¹⁰ C. Binet, D. F. Heaney, R. Spina, L. Tricarico: *J. Mater. Process. Technol.*, 164–165 (2005), 1160–1166
- ¹¹ Koza, J. R. *Genetic programming*; The MIT Press: Massachusetts, 1992
- ¹² Gen, M.; Cheng, R. *Genetic algorithms and engineering design*; John Wiley & Sons: Canada, 1997